Effects of Insulin Concentration and Self-Association on the Partitioning of Its A-21 Cyclic Anhydride Intermediate to Desamido Insulin and Covalent Dimer

Richard T. Darrington[1,2] and Bradley D. Anderson[1,3]

Received December 27, 1994; accepted February 9, 1995

Purpose. In the pH range 2–5, human insulin degrades via deamidation at the A-21 asn and covalent dimerization. Both products form via a common cyclic anhydride intermediate, a product of intramolecular nucleophilic attack by the A-21 carboxyl terminus. This study examines the influence of [insulin] and self-association on the partitioning of the intermediate to products. *Methods.* Insulin self-association was characterized (pH 2–4) by concentration difference spectroscopy. Deamidation rates (pH 2–4) and concurrent rates of covalent dimer formation (pH 4) were determined versus [insulin] at 35°C by initial rates. A mathematical model was developed to account for the overall rate and product composition profile versus pH and [insulin]. *Results.* Between pH 2–4, insulin self-associates to form non-covalent dimers with a pH independent association constant of $1.8 \times 10^4\ M^{-1}$. The overall rate of degradation is governed by intermediate formation, while product distribution is determined by competition between water and the phe B-1 amino group of insulin for the anhydride. In dilute solutions, deamidation is first-order in [insulin] while covalent dimerization is second-order. Thus, deamidation predominates in dilute solutions but the fraction of covalent dimer formed increases with [insulin]. At high [insulin], self-association inhibits covalent dimer formation, preventing exclusive degradation via this pathway. The model accurately predicts a maximum in covalent dimer formation near pH 4. *Conclusions.* A mechanism is described which accounts for the complex dependence of insulin's degradation rate and product distribution profile on pH (between 2–5) and [insulin]. If these results can be generalized, they suggest that covalent aggregation in proteins may be inhibited by self-association.

KEY WORDS: protein stability; insulin; insulin dimers; covalent aggregation; deamidation; chemical kinetics; intramolecular nucleophilic catalysis; self-association.

INTRODUCTION

Covalent aggregate formation is becoming increasingly recognized as a significant problem in the development of proteins as pharmaceutical products (1–7). Protein aggregates, whether physical or covalent, are a particular concern because of their role in the formation of precipitates in protein formulations (1, 2, 8), their reduced bioactivity (9) and their potential immunogenicity (10, 11).

We are particularly interested in conditions leading to the formation of covalent aggregates in proteins and the role of reactive intermediates in their formation. Because covalent dimer and higher oligomer formation most likely occur through bimolecular processes involving two protein molecules, covalent aggregation may become more problematic at high protein concentrations as encountered in extended-duration pharmaceutical formulations and in the solid-state (2). Protein self-association at high concentration may further significantly influence such processes either by sterically protecting reactive sites on one or both of the reactants or by bringing reactive sites into close proximity. Thus, obtaining a quantitative, mechanistic understanding of protein degradation is complicated by the existence of a diverse array of self-associated species in addition to protein monomer, each with its own characteristic reactivity.

Insulin serves as a useful model protein for examining the effects of concentration and self-association on covalent aggregate formation and for highlighting the potential importance of reactive intermediates in the nature of the reaction products formed under a variety of formulation conditions. Insulin undergoes both hydrolysis and covalent aggregate formation in solution and suspension dosage forms leading to a heterogeneous mixture of degradation products (12, 13). Covalent insulin dimers, which are present at low percentages in all types of insulin preparations, appear to form mainly through transamidation reactions and involve primarily, but not exclusively, the $asn_{A\text{-}21}$[4] and the $phe_{B\text{-}1}$ residues (14–18). Although covalent aggregates typically comprise a minor fraction of the overall degradation product fraction in a given formulation, their therapeutic impact is more serious. Covalent dimers accumulate in the circulation of type I diabetic patients undergoing prolonged insulin therapy and account for a significant proportion of the total insulin immunoreactivity (19). Some of the immunological side effects associated with insulin therapy may be due to the presence of covalent aggregates (15, 20, 21). Therefore, it is desirable that covalent dimer formation be minimized in pharmaceutical preparations.

In acidic solutions (pH 2–5), both insulin deamidation and covalent dimer formation proceed through a cyclic anhydride intermediate formed in the rate-limiting step via intramolecular nucleophilic catalysis by the protonated A-21 carboxyl terminus of insulin (17, 18). The partitioning of this anhydride intermediate to deamidated versus covalent dimer products most likely reflects the competition between two bimolecular processes involving nucleophilic attack by water or a second insulin molecule, respectively. Thus, high dilution would be expected to exclusively favor deamidation while concentrated insulin preparations would be expected to exhibit preferential formation of covalent dimer.

An added consideration which complicates prediction of the effects of insulin concentration on the degradation product profile is its tendency to self-associate in aqueous solution. In neutral insulin preparations, insulin exists largely in hexameric form (13, 22, 23). Brange has suggested (12) that covalent dimers form mainly within hexameric units because

[1] Department of Pharmaceutics and Pharmaceutical Chemistry, College of Pharmacy, University of Utah, Salt Lake City, Utah 84112.
[2] Present address: Glaxo Inc., Research Triangle Park, North Carolina 27709.
[3] To whom correspondence should be addressed.

[4] Unless otherwise noted, all amino acids mentioned are the L-enantiomers of the 20 commonly occurring amino acids and are referred to by their three letter abbreviations. X denotes an unspecified amino acid.

0724-8741/95/0700-1077$07.50/0

(a) covalent dimer formation appears to be independent of insulin concentration in neutral solutions, where hexamer predominates, and (b) covalent dimer formation decreases in the acidic pH range where insulin association is primarily dimeric (23). However, we have previously demonstrated that covalent dimers form even in solutions in which insulin is predominantly monomeric (18).

The purpose of this study was to elucidate the complex roles of insulin concentration and self-association on the partitioning of the A-21 cyclic anhydride intermediate to products. We characterized the self-association of insulin over the pH range of 2–4 by concentration difference spectroscopy. The effects of insulin concentration on deamidation and covalent dimer formation were carried out at pH 4 and interpreted in terms of the various insulin species present.

EXPERIMENTAL PROCEDURES

Materials. Unless otherwise noted all compounds were of reagent grade or higher purity and used as supplied. Chromatographic solvents were HPLC grade. Human Zinc Insulin (recombinant DNA origin), purchased either as the commercially available parenteral formulation Humulin® R U-100 from Eli Lilly & Co. or as a lyophilized powder from Miles Inc., was converted into a zinc free neutral solid (free base) as described elsewhere (24). The resulting lyophilized solid was stored desiccated at 4°C. Purity by RP-HPLC was >99% with the major impurity being [desamido$_{A\text{-}21}$] insulin. Karl Fischer moisture determination of this solid yielded an average water content of 5.4%. Solution concentrations reported in this study are uncorrected for moisture content of the solid.

[Desamido$_{A\text{-}21}$] human insulin was prepared from the above zinc free human insulin as described previously (24). Characterization was achieved by RP-HPLC coelution with a known reference sample of [desamido$_{A\text{-}21}$] human insulin generously provided by Dr. Ronald Chance of Eli Lilly & Co. The resulting amorphous solid was stored desiccated at 4°C. Purity by RP-HPLC was >99% with the major impurity being unmodified insulin.

Zinc free [desamido$_{A\text{-}21}$-phe$_{B\text{-}1}$] insulin dimer was isolated and characterized as described previously (18). The final apparent purity was >99% by RP-HPLC. We were unable to distinguish between α- and β-linked geometric isomers using this separation technique.

Characterization of the Self-Association Behavior of Zinc Free Human Insulin at Low pH Utilizing Concentration Difference Spectroscopy. Zinc free human insulin monomer-dimer association constants (K_{12}) were determined at low pH and 35°C using the method of concentration difference spectroscopy (25, 26). Ionic strength ($\mu = 0.1$) was controlled with sodium chloride. Concentration difference spectra were obtained using a dual beam scanning UV-Vis spectrophotometer equipped with calibrated 10 cm and 1 cm path length (±0.01 mm) quartz cuvettes. Water jacketed cell holders were constructed by the University of Utah department of engineering machine shop. Temperatures of the cell solutions were monitored with a calibrated micro temperature probe and controlled using a circulating water bath.

Fresh stock solutions of zinc free human insulin were prepared by carefully weighing an appropriate amount of insulin into 50 ml volumetric flasks and bringing to volume with the appropriate buffer, (pH 2.0-hydrogen chloride, pH 3.0-hydrogen chloride, pH 3.93-sodium acetate). Ionic strength was maintained ($\mu = 0.1$) with sodium chloride. Sample cell solutions were prepared from stock solution immediately prior to use. Reference cell solutions were prepared from the corresponding sample cell solution by carefully transferring a 5 ml aliquot using a class A volumetric pipette into 50 ml volumetric flasks and diluting to volume. Thus, for each sample solution prepared there was an exact 10-fold dilution prepared for the reference cell.

Difference spectra were generated using the following procedure: The 1 cm path length cell was placed in the sample beam and the 10 cm path length cell was placed in the reference beam. The appropriate buffer was added to both the sample and reference cells and allowed to come to thermal equilibrium after which a background correction scan was initiated to electronically correct for differences due to buffer. The more concentrated sample solution was then transferred into the 1 cm cell using a glass transfer pipette and immediately covered. The corresponding reference solution was similarly transferred into the 10 cm cell and immediately covered. After approximately 5 min both solutions had reached thermal equilibrium at 35°C and a difference spectrum was generated by scanning from 320 to 270 nm at 30 nm/min. Analysis of subsequent samples was achieved by draining the cuvettes with a glass transfer pipette, rinsing three times with the appropriate sample and filling. This procedure was used because removing, cleaning and drying the cells prior to filling resulted in significant fluctuations in the baseline. Utilizing the above procedure, the spectrophotometer subtracts the absorbance due to protein in the reference cell from the absorbance due to protein in the sample cell. Because the total number of insulin molecules in the path of the sample and reference beams are exactly equal ($c_s l_s = c_r l_r$), any difference spectrum generated should be the result of different fractions of associated and unassociated species in the sample and reference cells. ΔA values were recorded at the wavelength of maximum difference (285.5 nm) and plotted as a function of total insulin concentration in the sample cell (Ct_s).

The aforementioned method was validated by preparing a stock solution of potassium dichromate in 0.01M potassium hydroxide, which is known to exhibit concentration independent difference spectra (27). A corresponding 10-fold dilution of the potassium dichromate stock solution using the previously mentioned technique was performed and a concentration difference spectrum was generated from 500 to 220 nm at 30 nm/min. Absorbance differences observed were less than 0.0005 units.

Monomer-dimer equilibrium constants (K_{12}) were calculated from the absorbance differences using the following equation, which was adapted (17) from the work of Strazza (25,26):

$$\Delta A = \frac{\Delta\epsilon l_s}{4}\left\{\frac{1}{2K_{12}}\left(1-\frac{l_r}{l_s}\right) - \left[\left(4Ct_s + \frac{1}{2K_{12}}\right)^{1/2} - \left(\frac{l_r}{l_s}\right)\left(\frac{l_s}{l_r}4Ct_s + \frac{1}{2K_{12}}\right)^{1/2}\right]\left(\frac{1}{2K_{12}}\right)^{1/2}\right\} \quad (1)$$

where $\Delta\epsilon$ represents the difference in molar extinction coefficients between the monomer and dimer due to self-association, l_r and l_s are the path lengths of the reference and sample cells, respectively, and Ct_s is the total insulin concentration in the sample cell.

Kinetic Studies—Insulin Concentration Effects. Observed rate constants of [desamido$_{A\text{-}21}$] insulin formation (k_{obs}) were determined at pH 2.0 and 3.0, and concurrent rates of [desamido$_{A\text{-}21}$] insulin and [desamido$_{A\text{-}21}$-phe$_{B\text{-}1}$] dimer formation were determined as a function of total insulin concentration at pH 4.0 and 35°C using the method of initial rates, allowing no more than 10% of the starting material to react. Ionic strength (μ=0.1) was controlled with NaCl. Appropriate amounts of insulin were added to dichlorodimethylsilane (DCDMS) treated volumetric flasks (18) and diluted to volume with either 0.01M hydrogen chloride (pH 2.0), 0.01M sodium formate (pH 3.0), or 0.001M hydrogen chloride (pH 3.0) or 0.01 M acetate buffer (pH 4.0). Final insulin concentrations ranged from 3.76×10^{-6} to 8.60×10^{-4} M. The resulting solutions were then immediately transferred to DCDMS treated 2 ml or 4 ml vials in such a manner that there was a minimal air/water interface, tightly capped with Teflon rubber septa and placed in a circulating water bath at 35±0.1°C. Vials were removed at appropriate times and the reaction was quenched by chilling. Samples were stored at 4°C until analysis at which time insulin, [desamido$_{A\text{-}21}$] and [desamido$_{A\text{-}21}$-phe$_{B\text{-}1}$] dimer concentrations were determined as a function of time by RP-HPLC using a modular HPLC system described previously (18, 24) and a mobile phase containing 72.3% A (0.01 M ammonium sulfate adjusted to pH 2.0 with sulfuric acid) and 27.7% B (acetonitrile with 0.1% trifluoroacetic acid) or an initial mobile phase of 73% A and 27% B, and a gradient 1 min after injection (27% to 30% B at 0.13%/min, 30% to 35% B at 0.5%/min). Flow rate was 1.6ml/min with UV detection at 214 nm.

RESULTS

Concentration Difference Spectroscopy. A typical concentration difference spectrum generated for human insulin is shown in Figure 1. ΔA was determined graphically from the generated spectra by measuring the absorbance at 285.5 nm relative to the absorbance at 320 nm. Figure 2 depicts the relationship between ΔA and the total insulin concentration in the sample cell at pH 2.0, 3.0 and 3.93. Parameter values determined from fitting Equation (1) to the data in Figure 2 and their relative standard deviations are listed in Table I and indicate that over the pH range studied (2.00 to 3.93) K_{12} is virtually constant. The equilibrium constant for zinc free insulin association at pH 2.0 of 1.8×10^4 M^{-1} determined in this study is in excellent agreement with the value of 1.9×10^4 M^{-1} previously reported for bovine insulin under similar conditions (28).

Knowledge of K_{12} allows the calculation of the concentrations of insulin monomer and dimer, C_m and C_d, in terms of Ct:

$$Cm = \frac{-1 + \sqrt{1 + 8K_{12}Ct}}{4K_{12}} \quad (2)$$

$$Cd = 2K_{12}\left(\frac{-1 + \sqrt{1 + 8K_{12}Ct}}{4K_{12}}\right)^2 \quad (3)$$

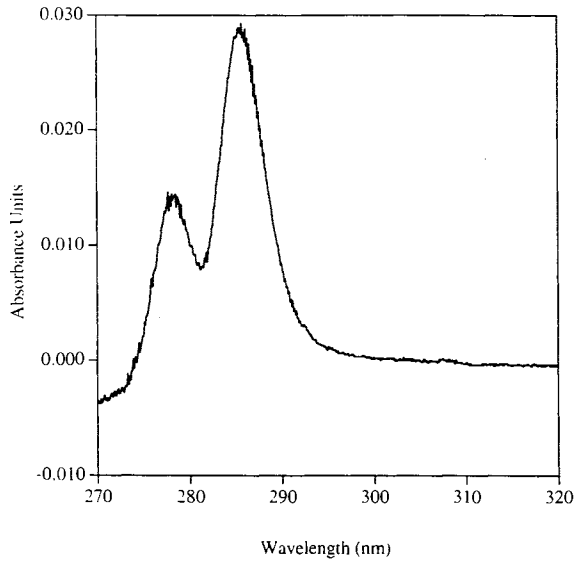

Fig. 1. Representative concentration difference spectrum for human insulin used to generate ΔA values versus insulin concentration. ΔA was determined graphically from the absorbance at 285.5 nm relative to that at 320 nm.

These calculated quantities were used in rationalizing the insulin decomposition product formation rates as a function of insulin concentration.

Effect of Self-Association on Insulin Decomposition. Plots of [desamido$_{A\text{-}21}$] and [desamido$_{A\text{-}21}$-phe$_{B\text{-}1}$] dimer concentration as a function of time were linear with respect to time over the course of the initial rate experiments. At pH 2.0 and 3.0, mass balance calculations indicated that the formation of [desamido$_{A\text{-}21}$] insulin completely accounted for the observed loss of insulin (i.e., covalent dimer formation was negligible). At pH 4.0 both [desamido$_{A\text{-}21}$] insulin and [desamido$_{A\text{-}21}$-phe$_{B\text{-}1}$] dimer formation were observed. Their

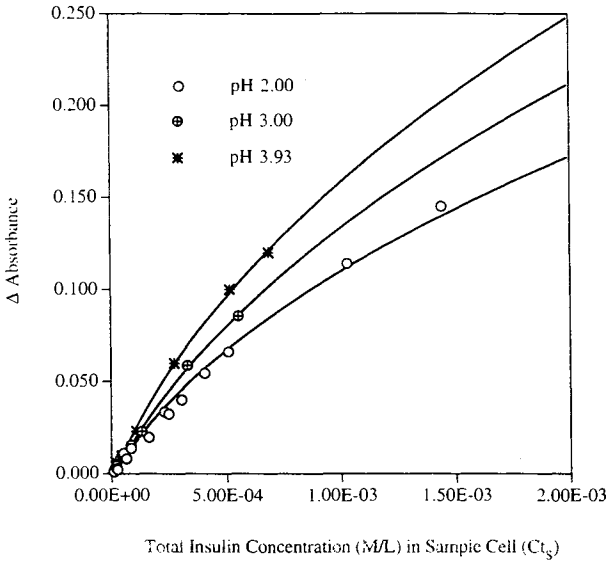

Fig. 2. ΔA as a function of total insulin concentration in the sample cell (Ct_s). Data shown were generated from concentration difference spectra at 35°C and pH 2.00, 3.00 and 3.93. The curves are nonlinear best fits of the data based on Eqn 1. Parameter values are listed in Table I.

Table I. Equilibrium Constants of Insulin Self-Association (i.e., Dimerization) by Concentration Difference Spectroscopy at 35°C and $\mu = 0.1$

pH	Buffer composition (0.01 M)	$\Delta\epsilon$ (M^{-1} cm^{-1})[a]	$K_{12} \times 10^{-4}$ (M^{-1})[a]
2.00	HCl	875.5 ± (37)	1.84 ± (0.2)
3.00	HCl[b]	987.5 ± (35)	1.46 ± (0.2)
3.93	Sodium acetate	1238.3 ± (59)	1.75 ± (0.4)

[a] Expressed as mean ± (standard deviation).
[b] 0.001 M HCl.

sum completely accounted for the observed loss of insulin over the duration of these experiments. The influence of total insulin concentration on the observed rate constants governing the overall decomposition (k_{obs}) of human insulin at pH 2.0, 3.0 and 4.0 and $\mu = 0.1$ (NaCl) was published previously (24). Insulin concentration has only a modest effect on the overall rate of insulin degradation over this pH range.

Rates of [desamido$_{A\text{-}21}$] insulin and [desamido$_{A\text{-}21}$-phe$_{B\text{-}1}$] dimer formation obtained as a function of insulin concentration were divided by total insulin concentration (C_t) to obtain apparent first-order rate constants, k_{des} and k_{dim}. These quantities are plotted versus C_t in Figure 3. At low insulin concentrations, where insulin monomer predominates (i.e., $C_t \leq 5 \times 10^{-5}$ M), k_{dim} increases with insulin concentration and, concurrently, k_{des} decreases. The relationship between k_{dim} and C_t asymptotically approaches a straight line as insulin concentration approaches zero, establishing the second order nature of covalent dimer formation in dilute solutions.

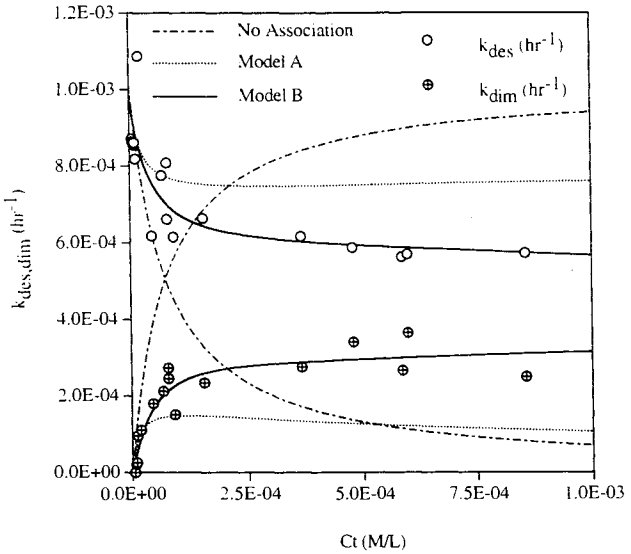

Fig. 3. Apparent first-order rate constants of [desamido$_{A\text{-}21}$] insulin formation (k_{des}) and [desamido$_{A\text{-}21}$-phe$_{B\text{-}1}$] dimer formation (k_{dim}) as a function of total insulin concentration (Ct) at pH 4.0 and 35°C. The solid curve is a non-linear least squares regression line based on Model B. The additional curves are simulations utilizing relevant parameter values generated from Model B but assuming either that insulin does not self-associate (–·–·–·–) or that the associated species are completely unreactive (. . .).

The decreases in k_{des} values with increasing k_{dim} suggest competition for the same intermediate, as depicted in Scheme I (left hand side) under conditions where the concentration of self-associated insulin dimer is negligible ($C_d \approx 0$).

If insulin did not self-associate, the changes in k_{des} and k_{dim} with increasing insulin concentration would follow the –·–·–·– line in Figure 3, with [desamido$_{A\text{-}21}$-phe$_{B\text{-}1}$] dimer formation becoming dominant at high C_t due to its 2nd order dependence on insulin concentration. The observed values illustrate that, contrary to these expectations, deamidation predominates even at high Ct, indicating that there is an attenuating effect, presumably due to insulin self-association, on [desamido$_{A\text{-}21}$-phe$_{B\text{-}1}$] dimer formation at high insulin concentrations. Moreover, k_{des} and k_{dim} approach plateaus at high insulin concentration with k_{des} remaining greater than k_{dim} over the entire concentration range.

Various models which take into account the effects of self-association on partitioning of the anhydride intermediate were considered to account for the results in Figure 3. Two of these, which are based on the reaction pathways illustrated in Scheme I, are described below. The first (Model A) assumes that only monomeric insulin species can react to form covalent dimer. The second (Model B) allows for all monomer-associated dimer reactions but precludes associated dimer-associated dimer reaction pathways. The additional curves in Figure 3 are based on these models, which are presented in detail in the following discussion.

Model A: Self-Association Prevents [desamido$_{A\text{-}21}$-phe$_{B\text{-}1}$] Formation. Based on the observation that increasing insulin concentration does not yield those increases in [desamido$_{A\text{-}21}$-phe$_{B\text{-}1}$] formation anticipated if self-association effects were negligible, this model assumes that insulin self-association completely inhibits [desamido$_{A\text{-}21}$-phe$_{B\text{-}1}$] formation. This assumption corresponds to setting the micro rate constants k_d, k'_m and k'_d equal to zero (Scheme I) and results in the following kinetic expressions:

$$k_{des} = \frac{k_{nuc}R_1[H_2O]Cm}{(R_1[H_2O] + Cm)Ct} + \frac{k'_{nuc}Cd}{Ct} \quad (4)$$

$$k_{dim} = \frac{k_{nuc}Cm^2}{(R_1[H_2O] + Cm)Ct} \quad (5)$$

where C_m, C_d, and C_t are the concentrations of monomer, dimer, and total insulin, respectively. k_{nuc} and k'_{nuc} represent the rate constants for the formation of the monomeric and self-associated anhydride intermediates, Anh and Anh', respectively, and R_1 is the ratio (k_1/k_m) of the rate constants for the formation of [desamido$_{A\text{-}21}$] insulin (k_1) and [desamido$_{A\text{-}21}$-phe$_{B\text{-}1}$] dimer (k_m) from the monomer anhydride intermediate. Since the formation and not the partitioning of the anhydride intermediate is rate-determining, only the ratio of k_1 to k_m could be determined and not the individual constants as these were highly correlated with each other. It is apparent from the curves in Figure 3 that this model underestimates the rate of [desamido$_{A\text{-}21}$-phe$_{B\text{-}1}$] formation with increasing insulin concentration, suggesting that self-association does not completely inhibit [desamido$_{A\text{-}21}$-phe$_{B\text{-}1}$] formation. However, it is important to note that at $C_t = 1.0 \times 10^{-3}$ M, where monomeric insulin is only 15% of the total insulin concentration, monomer-monomer reac-

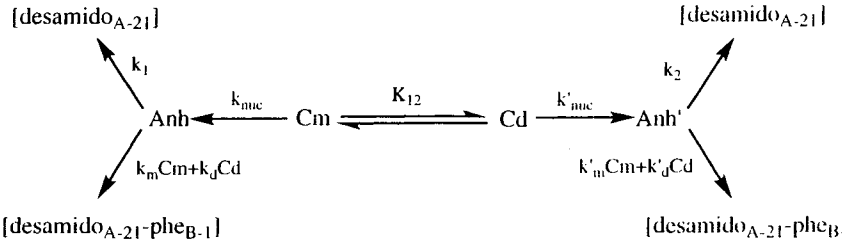

Scheme I. Kinetic scheme illustrating the formation of [desamido$_{A-21}$] insulin and [desamido$_{A-21}$-phe$_{B-1}$] dimer.

tions account for nearly half of the dimerization rate constant, k_{dim}. Thus, self-association inhibits covalent dimer formation.

Model B: Monomer-self-associated dimer reactions allowed. Excluding associated dimer-associated dimer collisions ($k'_d = 0$) but allowing all possible monomer-dimer collisions leads to the following kinetic expressions:

$$k_{des} = \frac{k_{nuc}R_1[H_2O]Cm}{(R_1[H_2O]+R_3Cm+Cd)Ct} + \frac{R_2[H_2O]k'_{nuc}Cd}{(R_2[H_2O] + Cm)Ct} \quad (6)$$

$$k_{dim} = \frac{k_{nuc}Cm(R_3Cm + Cd)}{(R_1[H_2O] + R_3Cm + Cd)Ct} + \frac{k'_{nuc}CmCd}{(R_2[H_2O] + Cm)Ct} \quad (7)$$

where R_1 ($= k_1/k_d$) represents the relative reactivity of water and associated insulin dimer towards the monomer anhydride, R_2 ($= k_2/k'_m$) represents the relative reactivity of water and insulin monomer towards the associated anhydride, and R_3 ($= k_m/k_d$) is the relative reactivity of insulin monomer and associated insulin dimer toward the monomer anhydride. Nonlinear regression analyses of the data according to the above equations resulted in an excellent fit, as illustrated by the solid curves in Figure 3, indicating that monomer-monomer and monomer-dimer collisions are sufficient to explain the observed rates of deamidation and covalent dimer formation as a function of insulin concentration. Parameter values generated by fitting Model B to the data are listed in Table II.

DISCUSSION

Self-Association of Zinc Free Human Insulin at Low pH. The pH dependence of the self-association of zinc free human insulin was determined at 35°C and at an ionic strength of 0.1 using the method of concentration difference spectroscopy described by Strazza (25, 26). An increase in the extinction coefficient ($\Delta\epsilon$) occurs on insulin self-association most likely due to changes in the microenvironment of tyrosine residues near the interface upon association (29). Similarly, the observed increases in $\Delta\epsilon$ with increasing pH may be ascribed to environmental differences in the tyrosine side chains brought about by changes in pH (26, 28, 29).

Table II. Parameter Values Describing [desamidoA-21] and [desamidoA-21-pheB-1] Formation as a Function of Total Insulin Concentration at pH 4.0 According to Model B (Eqns. 6 & 7) Generated by Non-linear Regression Analysis

Parameter	Value	SDev
knuc ($hr^{-1} \times 10^4$)	9.7	0.7
k'_{nuc} ($hr^{-1} \times 10^4$)	8.7	0.6
R_1 ($\times 10^6$)	1.54	1.16
R_2 ($\times 10^6$)	8.9	2.6
R_3	0.48	1.0

[a] $R_1 = k_1/k_d$.
[b] $R_2 = k_2/k'_m$.
[c] $R_3 = k_m/k_d$.

The changes in concentration difference spectra with insulin concentration obtained in this study are well described by a simple monomer-dimer association (Eq. 1). Lord et al. (28) took into account the formation of insulin oligomers larger than the dimer in their concentration difference studies of zinc bovine insulin and observed no significant improvement over the assumption of a monomer-dimer equilibrium model at pH 2.0 and 3.5. This is in agreement with the weak association of zinc insulin from dimer to higher order oligomers observed by Jeffrey and Coates (30). At a concentration of 2 mg/ml (pH 2.0, 25°C, $\mu = 0.1$), zinc insulin is approximately 80% dimer with less than 10% tetramer and negligible amounts of hexamer (30). Zinc ions are not involved in dimer formation but are involved in hexamer formation (23, 31–33). Thus, it can be argued that the amount of higher order oligomers in zinc free insulin solutions would be significantly less than in insulin solutions containing zinc. This is supported by the work of Goldman and Carpenter (34) who found that at pH 8.0 in the absence of zinc, dimer formation is much stronger than tetramer or hexamer formation. We conclude that under the conditions of this study (zinc free, pH 2.0–3.93) only negligible amounts of tetramer and hexamer would be expected to be present and these species were therefore neglected in our theoretical treatment of the data.

Jeffrey and Coates (35) proposed that increasing the overall charge of the insulin molecule would inhibit self-association due to charge-charge repulsion. The net charge of human insulin (pI = 5.4) decreases slightly from pH 2.00 to 3.93 and, based on the arguments of Jeffrey and Coates, self-association should increase. However, crystallographic studies (23, 36, 37) indicate that only non-polar residues and a series of hydrogen bonds forming an anti-parallel beta sheet are involved in the dimerization of insulin, neither of which should be extremely sensitive to changes in pH. This may explain why we observed no significant difference in the dimerization constant of zinc-free insulin between pH 2–4 (Table I).

Effects of Self-Association on Insulin Decomposition and Anhydride Partitioning. Insulin self-association alters both the rate-limiting step of its decomposition over pH 2–5

(i.e., cyclic anhydride formation) and the subsequent partitioning of the reactive intermediate to products. The effects of insulin self-association on its overall decomposition rate, reported in a previous paper (24), are relatively small. We observed a modest (2.5-fold) enhancement in the reactivity of the A-21 asparagine in insulin in the self-associated dimer. Accompanying this change, however, is an apparent downward shift in the pKa of the asn_{A-21} carboxylic acid group of approximately 0.7 units upon self-association. At pH 4 these two effects nearly cancel so that the overall rate of insulin decomposition is nearly independent of insulin concentration. These modest effects of self-association may reflect the fact that formation of a cyclic anhydride intermediate involves intramolecular nucleophilic attack of a carboxyl substituent in close proximity to the asn_{A-21} amide linkage, a reaction which may occur in a microenvironment which is not altered dramatically upon self-association. Moreover, several groups have demonstrated that only minor conformational changes occur in monomeric subunits upon insulin self-association (38–40). These minor structural perturbations result in the formation of a loose contact between thr_{B-27} of molecule 1 and the asn_{A-21} amide of molecule 2. Subsequent association of dimers to form hexamers does not further affect the asn_{A-21} residues (36).

While the observed effects of insulin self-association on the overall rate of insulin degradation are small, insulin concentration has a more pronounced influence on the nature of the products formed. With increasing insulin concentration, covalent dimer formation should increasingly predominate over deamidation because the former reaction is second-order in insulin concentration while the latter is first-order. For these reasons, covalent dimer/higher aggregate formation in proteins would, in general, be expected to become increasingly problematic at high protein concentrations.

Contrary to predictions based on considering reaction order alone, [desamido$_{A-21}$-phe$_{B-1}$] dimer formation does not become dominant with increasing insulin concentration but rather is attenuated by self-association, as is evident in Figure 3. On the other hand, the apparent first-order rate constants for both [desamido$_{A-21}$] and [desamido$_{A-21}$-phe$_{B-1}$] formation approach plateau values at high insulin concentration which are significantly above the predictions of Model A, which assumes that covalent dimer formation is completely inhibited by self-association. Thus, kinetic schemes which include participation of self-associated insulin in covalent dimer formation must be considered.

The simplest model consistent with the results is Model B, which assumes that [desamido$_{A-21}$-phe$_{B-1}$] dimer formation may occur via monomer-monomer and monomer-associated dimer reactions, and that covalent dimer formation does not occur through reactions between or within self-associated dimers.

Brange et al. (15) investigated the kinetics of covalent aggregation of commercial insulin formations ranging in concentration from 1.5 mg/ml (40 IU) to 3.8 mg/ml (100 IU). Based on the observation that the rate of dimer formation was constant over this concentration range they proposed that insulin covalent aggregation occurs only within the associated hexamer units. However, results of the present study conclusively demonstrate that covalent dimer formation involves primarily insulin monomers with a smaller contribution from self-associated insulin. Thus, insulin self-association significantly reduces insulin covalent aggregation but does not preclude it.

The sites involved in the chemical reactivity of human insulin at low pH (asn_{A-21} and phe_{B-1}) remain relatively unprotected in the associated dimer suggesting that specific effects of self-association on reactivity may be minimal (13, 23, 36, 37, 41). This seems particularly likely to be the case in the reaction of the A-21 cyclic anhydride with water, where the accessibility of this site to water may be unaffected by self-association. Inhibition of covalent dimer formation by self-association may be the result of steric effects hindering the approach of the phe_{B-1} of a self-associated insulin dimer to the cyclic anhydride group within another self-associated dimer molecule.

Comprehensive Model for Insulin Degradation at Low pH. We have described in this paper a mathematical model to account for the partitioning of the cyclic anhydride intermediate of insulin to desamido insulin and covalent dimer as a function of insulin concentration in the pH range where insulin self-association involves primarily self-associated dimers. In previous publications, we have similarly accounted for the effects of pH between 2–5 (18, 24). These combined publications contain virtually all of the necessary information to develop a comprehensive mathematical model describing the degradation of insulin as a function of pH and insulin concentration over the pH range where decomposition is mediated through cyclic anhydride intermediate formation.

Figures 4a & b display the results of model calculations for the percentages of [desamido$_{A-21}$] insulin (% Des A-21) and [desamido$_{A-21}$-phe$_{B-1}$] dimer (% A-B dimer) formed after 32 hours at 35°C as a function of pH and insulin concentration. At low insulin concentration, deamidation dominates over the entire pH range, but decreases with increasing pH in response to the decreasing concentration of the catalytic A-21 carboxyl in unionized form. The observed % A-B dimer formation increases with insulin concentration and exhibits a sharp maximum near pH 4. Indeed, at high insulin concentration and above pH 4, covalent dimer formation predominates.

The maximum in % A-B dimer at pH 4 is in close agreement with observations by Brange et al. (42) and Markussen et al. (43) on commercial insulin products. The model predicted maximum may be rationalized in the following way. At pH < 4, increasing pH increases the fraction of cyclic anhydride reacting with the phe B-1 amine of a second molecule of insulin in large part due to the increased fraction of unionized amine, resulting in a rise in % A–B dimer with increasing pH. A second consequence of the increased ability of the phe B-1 amino group in insulin to compete with water for nucleophilic attack on the anhydride is the steep decline in % Des A-21 vs. pH at high insulin concentration (Figure 4a). The decline in % A–B dimer from its maximum as pH continues to increase reflects two contributions: (a) the overall reactivity of insulin to form cyclic anhydride decreases with increasing pH; and (b) the nucleophilic attack of the phe B-1 amino on the anhydride intermediate plateaus with increasing pH, even at pH values significantly below the pKa of this group, due to the influence of neighboring ionizable groups in the reactants (18).

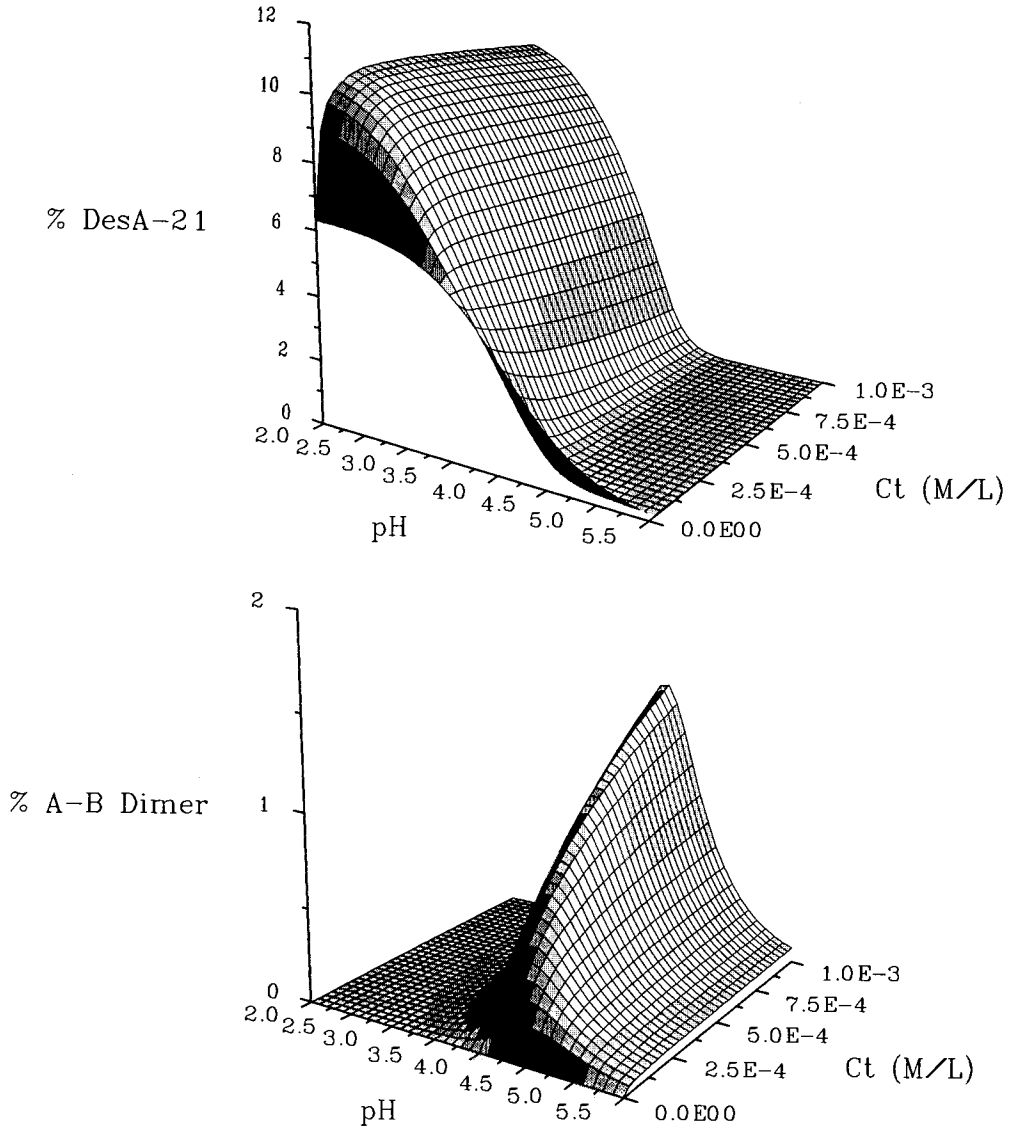

Fig. 4. (a) Comprehensive model calculated percentage of [desamido$_{A\text{-}21}$] insulin (% Des A-21) formed in zinc-free human insulin solutions as a function of pH and total insulin concentration after 32 hr at 35°C. (b) Comprehensive model calculated percentage of [desamido$_{A\text{-}21}$-phe$_{B\text{-}1}$] dimer (% A–B dimer) formed from zinc free human insulin as a function of pH and concentration after 32 hr at 35°C.

The predictions obtained from this comprehensive, mechanism-based mathematical model illustrate the value in accounting for the reactivities of the various molecular species which exist in a given protein formulation. The mechanism and the model derived from it explain both the pH and concentration effects on overall insulin reactivity and the product distribution profiles versus pH and concentration. In a subsequent paper, we will take advantage of this mechanistic understanding to explore the reactivity of insulin in the lyophilized state over the same apparent pH range.

ACKNOWLEDGMENTS

This work was made possible in part by a Merck/INTERx Pre doctoral Fellowship and a Parenteral Drug Association Foundation for Pharmaceutical Sciences, Inc. grant in biotechnology.

REFERENCES

1. B. M. Eckhardt, J. Q. Oeswein, T. A. Bewley. Effect of freezing on aggregation of human growth hormone. *Pharm. Res.* 8:1360–1364 (1991).
2. M. J. Hageman, J. M. Bauer, P. L. Possert, R. T. Darrington. Preformulation studies oriented toward sustained delivery of recombinant somatotropins. *J. Agric. Food Chem.* 40:348–355 (1992).
3. M. S. Hora, R. K. Rana, F. W. Smith. Lyophilized formulations of recombinant tumor necrosis factor. *Pharm. Res.* 9:33–36 (1992).
4. R. Pearlman, T. A. Bewley. Stability and Characterization of human growth hormone. In Wang YJ, Pearlman R, Eds. *Stability and Characterization of Protein and Peptide Drugs: Case Histories*. Plenum Press, New York, 1993, 1–58.
5. M. W. Townsend, P. P. DeLuca. Nature of aggregates formed during storage of freeze-dried ribonuclease A. *J. Pharm. Sci.* 80:63–66 (1991).
6. L. C. Gu, E. A. Erdos, H.-S. Chiang, T. Calderwood, K. Tsai,

G. C. Visor, J. Duffy, W.-C. Hsu, L. C. Foster. Stability of interleukin 1β (IL-1β) in aqueous solution: analytical methods, kinetics, products, and solution formulation implications. *Pharm. Res.* 8:485–490 (1991).
7. S. Yoshioka, Y. Aso, K. Izutsu, T. Terao. Stability of β-galactosidase, a model protein drug, is related to water mobility as measured by ^{17}O nuclear magnetic resonance (NMR). *Pharm. Res.* 10:103–108 (1993).
8. L. Gu, J. Fausnaugh. Stability and characterization of human interleukin-1β. In Wang YJ, Pearlman R, ed. *Stability and Characterization of Protein and Peptide Drugs*. Plenum Press, New York, 1993, 221–248.
9. G. W. Becker, R. R. Bowsher, W. C. Mackellar, M. L. Poor, P. M. Tackitt, R. M. Riggin. Chemical, physical, and biological characterization of biosynthetic human growth hormone. *Biotech. Appl. Biochem.* 9:478–487 (1987).
10. C. Rougeot, P. Marchand, F. Dray, J. C. Job, M. Pierson, C. Ponte, P. Rochiccoili, R. Rappaport. Comparative study of biosynthetic human growth hormone immunogenicity in growth hormone deficient children. *Horm. Res.* 35:76 (1991).
11. W. V. Moore, P. Leppert. Role of aggregated human growth hormone in development of antibodies to human growth hormone. *J. Clin. Endocrinol. Metab.* 51:691–697 (1980).
12. J. Brange, L. Langkjaer. Insulin structure and stability. In Wang YJ, Pearlman R, ed. *Stability and Characterization of Protein and Peptide Drugs: Case Histories*. Plenum Press, New York, 1993, 315–350.
13. J. Brange. *Galenics of Insulin: The physico-chemical and Pharmaceutical aspects of insulin and insulin preparations*. Springer-Verlag. New York, 1987.
14. H.-J. Helbig. Insulindimere Aus Der B-Komponente Von Insulinpraparationen [Dissertation]. Rheinisch-Westfalischen Technischen Hochschule, Aachen, 1976.
15. J. Brange, S. Havelund, P. Hougaard. Chemical Stability of Insulin. 2. Formation of Higher Molecular Weight Transformation Products During Storage of Pharmaceutical Preparations. *Pharm. Res.* 9:727–734 (1992).
16. J. Brange, O. Hallund, E. Sorensen. Chemical Stability of Insulin 5. Isolation, Characterization and Identification of Insulin Transformation Products. *Acta Pharm. Nord.* 4:223–232 (1992).
17. R. T. Darrington. The Role of Self-Association and Intramolecular Catalysis in the Chemical Stability of Human Insulin at low pH. [Ph.D. Dissertation]. University of Utah, 1993.
18. R. T. Darrington, B. D. Anderson. Evidence for a Common Intermediate in Insulin Deamidation and Covalent Dimer Formation: Effects of pH and Aniline Trapping in Dilute Acidic Solutions. *J. Pharm. Sci.* 84:275–282 (1995).
19. M. Maislos, P. M. Mead, D. H. Gaynor, D. C. Robbins. The Source of the Circulating Aggregate of Insulin in Type I Diabetic Patients is Therapeutic Insulin. *J. Clin. Invest.* 77:717–723 (1986).
20. R. E. Ratner, T. M. Phillips, M. Steiner. Persistent cutaneous insulin allergy resulting from high-molecular-weight insulin aggregates. *Diabetes.* 39:728–733 (1990).
21. D. C. Robbins, S. M. Cooper, S. E. Fineberg, P. M. Mead. Antibodies to covalent aggregates of insulin in blood of insulin-using diabetic patients. *Diabetes.* 36:838–841 (1987).
22. J. F. Hansen. The Self-association of Zinc-free Human Insulin and Insulin Analogue B13-glutamine. *Biophys. Chem.* 39:107–110 (1991).
23. T. Blundell, G. Dodson, D. Hodgkin, D. Mercola. Insulin: The Structure in the Crystal and Its Reflection in Chemistry and Biology. *Adv. Protein Chem.* 26:279–402 (1972).
24. R. T. Darrington, B. D. Anderson. The Role of Intramolecular Nucleophilic Catalysis and the Effects of Self-Association on the Deamidation of Human Insulin at Low pH. *Pharm. Res.* 11:784–793 (1994).
25. S. Strazza. The Thermodynamics of Association of the Insulin Dimer. [Ph. D. Dissertation]. New Mexico State University, 1976.
26. S. Strazza, R. Hunter, E. Walker, D. W. Darnall. The Thermodynamics of Bovine and Porcine Insulin and Proinsulin Association Determined by Concentration Difference Spectroscopy. *Arch Biochem. Biophys.* 238:30–42 (1985).
27. G. W. Haupt. An Alkaline Solution of Potassium Chromate as a Transmittancy Standard in the Ultraviolet. *J. Res. Nat. Bur. Stnds.* 48:414–423 (1952).
28. R. S. Lord, F. Gubensek, J. A. Rupley. Insulin Self-Association. Spectrum Changes and Thermodynamics. *Biochem.* 12: 4385–4391 (1973).
29. D. B. Wetlaufer. Ultraviolet of Proteins and Amino Acids. *Advan. Protein Chem.* 17:303–390 (1962).
30. P. D. Jeffrey, J. H. Coates. An Equilibrium Ultracentrifuge Study of the Effect of Ionic Strength on the Self-Association of Bovine Insulin. *Biochem.* 5:3821–3824 (1966).
31. D. Smith, D. C. Swenson, E. J. Dodson, G. G. Dodson, C. D. Reynolds. Structural Stability in the 4-Zinc Human Insulin Hexamer. *Proc. Natl. Acad. Sci. USA.* 81:7093–7097 (1984).
32. D. T. Manallack, P. R. Andrews, E. F. Woods. Design, Synthesis, and Testing of Insulin Hexamer-Stabilizing Agents. *J. Med. Chem.* 28:1522–1526 (1985).
33. F. D. Coffman, M. F. Dunn. Insulin-Metal Ion Interactions: The Binding of Divalent Cations to Insulin Hexamers and Tetramers and the Assembly of Insulin Hexamers. *Biochem.* 27:6179–6187 (1988).
34. J. Goldman, F. H. Carpenter. Zinc Binding, Circular Dichroism, and Equilibrium Sedimentation Studies of Insulin (Bovine) and Several of Its Derivatives. *Biochem.* 13:4566–4574 (1974).
35. P. D. Jeffrey, J. H. Coates. An Equilibrium Ultracentrifuge Study of the Self-Association of Bovine Insulin. *Biochem.* 5:489–498 (1966).
36. E. N. Baker, T. L. Blundell, J. F. Cutfield, S. M. Cutfield, E. J. Dodson, G. G. Dodson, D. M. C. Hodgkin, R. E. Hubbard, N. W. Isaacs, C. D. Reynolds, K. Sakabe, N. Sakabe, N. M. Vijayan. The Structure of 2Zn Pig Insulin Crystals at 1.5 A Resolution. *Phil. Trans. R. Soc. Lond. B.* 319:369–456 (1988).
37. T. L. Blundell, J. F. Cutfield, S. M. Cutfield, E. J. Dodson, G. G. Dodson, D. C. Hodgkin, D. A. Mercola. Three-Dimensional Atomic Structure of Insulin and Its Relationship to Activity. *Diabetes.* 21(Suppl. 2):492–505 (1972).
38. R. Palmieri, R. W. Lee, M. F. Dunn. ^1H Fourier Transform NMR Studies of Insulin: Coordination of Ca^{2+} to the Glu(B13) Site Drives Heaxmer Assembly and Induces a Conformation Change. *Biochem.* 21:3387–3397 (1988).
39. M. Roy, R. W. K. Lee, J. Brange, M. F. Dunn. ^1H NMR Spectrum of the Native Human Insulin Monomer: Evidence for Conformational Differences between the Monomer and Aggregated Forms. *J. Biol. Chem.* 265:5448–5452 (1990).
40. A. E. Mark, H. J. C. Berendesn, W. F. V. Gunstrten. Conformational Flexibility of Aqueous Monomeric and Dimeric Insulin: A Molecular Dynamics Study. *Biochem.* 30:10866–10872 (1991).
41. F. H. Carpenter. Relationship of Structure to Biological Activity of Insulin as Revealed by Degradative Studies. *Amer. J. Med.* 40:750–758 (1966).
42. J. Brange, L. Langkjaer. Chemical Stability of Insulin. 3. Influence of Excipients, Formulation, and pH. *Acta Pharm. Nord.* 4:149–158 (1992).
43. J. Markussen, I. Diers, P. Hougaard, L. Langkjaer, K. Norris, L. Snel, A. R. Sorensen, E. Sorensen, H. O. Voigt. Soluble Prolonged-Acting Insulin Derivatives. III. Degree of Protraction, Crystallizability and Chemical Stability of Insulins Substituted in Positions A21, B13, B23, B27 and B30. *Prot. Engineer.* 2:157–166 (1988).